Proceedings of the 17th World Congress
The International Federation of Automatic Control
Seoul, Korea, July 6-11, 2008

Simultaneous Design and Control of the Tennessee Eastman Process

Luis A. Ricardez-Sandoval*. Hector M. Budman**
Peter L. Douglas***

**University of Waterloo, Waterloo, ON N2L 3G1*
Canada (Tel: 519-888-4567; email: laricard@uwaterloo.ca).
***email:hbudman@uwaterloo.ca*
****email:pdouglas@uwaterloo.ca*

Abstract: This paper presents a large-scale application of a new approach to simultaneously design and control chemical processes that does not require dynamic programming and a priori assumptions of the disturbance dynamics. The process closed-loop behavior is represented as a state space uncertain model. The robust models are then used to calculate infinite-time horizon bounds on the process stability, worst-case variability and process constraints using a Singular Structured Value (SSV) approach. The proposed methodology was used to simultaneously design and control the Tennessee Eastman Process.

1. INTRODUCTION

Chemical processes have been traditionally designed by considering only the process steady-state behaviour together with process synthesis heuristics. Although this approach may produce an economically attractive design, it is *assumed* that a suitable control structure for this system can be specified such that it would keep the process within constraints. However, the effect of external perturbations and process parametric uncertainties often result in unfavourable process dynamics that limits the controller performance in such a way that it could drive the system to an operating region in which the design goals cannot be met. As a result, researchers have decided to consider the controllability and resiliency aspects of the process at the design stage. Due to its complexity, several attempts have been made to tackle this problem. Several studies have proposed a dynamic optimization approach using a single performance index cost function. Since these methods use the complete process nonlinear dynamic model together with advanced control techniques, an intensive computational effort is required to attain the design of chemical processes with a small number of process units; thus, its application to large-scale processes is limited by this fact. A comprehensive review of these methodologies is given in Seferlis and Georgiadis (2004) and Sakizlis et al. (2004). Recently, Chawankul et al. (2007) proposed a parameterized model-based approach that applies robust control measures to assess the design whereas Gerhard et al. (2006) proposed an approach that explores the space of uncertain parameters to build critical boundaries over the process stability and feasibility regions. Although these methods avoid the task of solving dynamic optimization problems, they require a priori specification of the disturbance dynamics.

The aim of this paper is to present a robust modelling approach-based methodology and its application to a large-scale benchmark process: the Tennessee Eastman Process (TEP). The proposed methodology addresses the integration of design and control problem by borrowing analytical tools from robust control theory and do not require a priori assumption of the perturbation dynamics. Although the TEP has been widely used to study different process system engineering areas, to our knowledge, this is the first paper that provides insight regarding the design of this plant.

2. MATHEMATICAL FORMULATION

The methodology applied to simultaneously design and control the TEP was proposed by Ricardez Sandoval et al. (2007) and is explained in this section.

2.1 Cost Function

The objective function to be minimized is defined as follows:

$$O.F. = \mathrm{CC}\left(\mathbf{d}, \bar{\mathbf{u}}\right) + \mathrm{OP}\left(\mathbf{d}, \bar{\mathbf{u}}\right) + \mathrm{VC}\left(\mathbf{d}, \bar{\mathbf{u}}, \boldsymbol{\lambda}, \varphi^{y}\right) \quad (1)$$

Where *CC*, and *OP*, and *VC* refer to the process capital, operating and variability costs whereas **d** and **u** denotes the process design and available manipulated variables, respectively. The variable $\bar{\mathbf{u}}$ in (1) denotes a nominal steady-state value for **u** while $\boldsymbol{\lambda}$ denotes the controller tuning parameters. The capital and operating costs can be estimated from cost correlation functions that usually depend on the values specified for **d** and $\bar{\mathbf{u}}$. The function φ^{y} represents the process variability, which is problem specific and is defined based on the goals to attain by the design. For example, if the goal is to design a process whose product lies within 99.9% of spec at all time, then the process variability may be defined as the difference between the product spec at steady-state and the true product spec obtained when external perturbations and parametric uncertainties are affecting the process. This deviation from product specifications must be

accepted to remain within the design targets. The cost related to this difference, e.g. lost profit, will be the process variability cost.

2.2 Disturbances.

A set of disturbances with bounded amplitude and any given bandwidth can be considered, i.e., $\boldsymbol{\upsilon}=\{\ \upsilon_q^{\,l} \le \upsilon_q \le \upsilon_q^{\,u}\ \}$, where υ_q denotes the q^{th} disturbance value at any time t and $\boldsymbol{\upsilon}$ is a vector whose length is determined by the number of the disturbances (m) considered in the design.

2.3 Robust closed-loop process model.

The present approach assumes that a closed-loop process model is available to simulate the process dynamics. The main idea in this work is to represent the true process closed-loop model by a linear state space model complemented with model parameter uncertainty (θ), as follows:

$$\begin{aligned}\dot{\mathbf{x}} &= \mathbf{A}(\theta_A)\mathbf{x} + \mathbf{B}(\theta_B)\boldsymbol{\upsilon} \\ \mathbf{y} &= \mathbf{C}(\theta_C)\mathbf{x} + \mathbf{D}(\theta_D)\boldsymbol{\upsilon}\end{aligned} \tag{2}$$

Each element of the state space matrices in (2) is bounded between a lower and an upper bound, i.e. $a_{i,i}\pm\theta_{ij}$. Since $\boldsymbol{\upsilon}$ is the only input in (2), the uncertain parameters (θ) will capture only the process nonlinearities due to changes in this variable. Robust models like (2) can be obtained as follows: based on the process open-loop time constant, an excitation signal, i.e. PRBNS, is designed for $\boldsymbol{\upsilon}$ using the lower and upper bounds of this variable and used to simulate the process transient behaviour. The input/output data collected from simulation is then fitted to a linear transfer function model using the least squares method (Ljung, 1987). This model is transformed into a canonical state space model via a state space realization. The covariance matrix generated from the linear parameter identification is then used to estimate the uncertain model parameters (θ). The robust model shown in (2) is only valid around a region of nominal operating conditions, specified by the steady-state values of the manipulated variables ($\bar{\mathbf{u}}$) and the process output variables ($\bar{\mathbf{y}}$), the design variables (**d**), and the controller tuning parameters ($\boldsymbol{\lambda}$). Thus, the closed loop model has to be re-identified around each new set of nominal conditions arising during the optimization. Additional models with the structure in (2) can also be used to describe the behaviour between $\boldsymbol{\upsilon}$ and a process output variable (**y**) or a manipulated variable (**u**) for example. Then, these robust models can also be used to test constraints on these different process variables.

2.4 Process stability.

The present method applies a quadratic Lyapunov function-based approach to test process stability. A linear time invariant system like (2) is asymptotically stable if there is a quadratic Lyapunov function $V(x)=\mathbf{x}^T\mathbf{Q}\mathbf{x}$ such that $\mathbf{A}(\theta_A)^T\mathbf{Q}+\mathbf{Q}\mathbf{A}(\theta_A)<0$ with $\mathbf{Q}$ being a positive definite symmetric matrix (Boyd and Yang, 1989). This set of infinite inequalities can be reduced, due to the convexity in *V(x)*, to a finite set of linear matrix inequalities (LMI's), evaluated at the vertexes of an hyperrectangle formed with the extreme values of the $\mathbf{A}(\theta_A)$ state space matrix. The finite set of LMI's can be posed as follows:

$$\begin{aligned}&\mathbf{A}(w_k)^T\mathbf{Q}+\mathbf{Q}\mathbf{A}(w_k)<0 \quad for \quad all\ w_k \in \mathbf{W} \\ &\mathbf{W}=\left\{\left(w_1,w_2,\ldots,w_n\right): w_k \in \left[a_{ij}-\theta_{A,ij}, a_{ij}+\theta_{A,ij}\right]\right\}\end{aligned} \tag{3}$$

Where w_k represents the k^{th} vertex of the hyper-rectangle. Inequality (3) is included as a constraint within the optimization to guarantee that the design attained by this method is asymptotically stable. Future work in this research will be focused on reducing the conservatism in (3) by the use of parameter-dependent Lyapunov functions.

2.5 Worst-case variability.

The major challenge faced when integrating design and control is to determine the critical time profile in the disturbance that generates the largest process output variability around a nominal operating point. This condition, often referred to as the worst-case variability, is either estimated by dynamic programming (e.g. Sakizlis et al. 1996) or specified a priori (e.g. Gerhard et al. 2006). The present method estimates the critical profile in $\boldsymbol{\upsilon}$ that produces the largest output variability as well as a bound on this condition by solving a Singular Structured Value (SSV) problem. To assess the worst-case variability, a robust finite impulse response model (FIR) as shown below is required:

$$\mathrm{y(j)}=\sum_{q=1}^{m}\sum_{i=0}^{j}\left[h_{iq}\delta\upsilon_q(j-i)+\delta h_{iq}\delta\upsilon_q(j-i)\right],\ 0\le j\le N \tag{4}$$

Where $\delta\upsilon_q$ denotes a maximal rate of change of the q^{th} disturbance, defined as $\delta\upsilon_q=(\upsilon_q^{\,l}-\upsilon_q^{\,u})/2$. This variable represents the range of values that υ_q may take at any time step j. The impulse response coefficients nominal values (h_{iq}) and their corresponding uncertainties (δh_{iq}) are calculated as follows:

$$h_{iq}=\left(h_{iq}^{\,l}+h_{iq}^{\,u}\right)/2;\ \delta h_{iq}=\left(h_{iq}^{\,l}-h_{iq}^{\,u}\right)/2 \tag{5}$$

Where $h_{iq}^{\,l}$ and $h_{iq}^{\,u}$ denote the lower and upper bounds of **y** at each time step j for each υ_q. Since it is assumed that the system to be designed is a continuous process, (4) will be obtained for a predetermined time horizon, specified by the output's settling time, N. Model (4) can be obtained from (2) as follows: assuming that the vertexes of the hyperrectangle formed with the extreme values of each of the models

uncertain parameters shown in (2) are used, a unit pulse is imposed on each υ_q to simulate (2) which generate a finite set of FIR models. The values of $h_{iq}{}^u$ and $h_{iq}{}^l$ are obtained from the search of the maximum and minimum values among the FIR models at each time step *j*. Based on the above, the worst-case variability can thus be defined as follows:

$$\max_{\upsilon_q \in \boldsymbol{\upsilon}} \left| y(j) \right| \tag{6}$$

The above problem cannot be solved analytically but a bound can be obtained by rewriting (6) in terms of a Mixed Singular Structured Value problem (Nagy and Braatz, 2003). For any real *k*:

$$\max_{\upsilon_q \in \boldsymbol{\upsilon}} \left| \sum_{q=1}^{m} \sum_{i=0}^{j} \left[h_{iq} \delta \upsilon_q (j-i) + \delta h_{iq} \delta \upsilon_q (j-i) \right] \right| \geq k \Leftrightarrow \max_{\mu_{\boldsymbol{\Delta}}(\mathbf{M}) \geq k} k \tag{7}$$

The problem posed in the RHS of (7) is known as a skewed-μ calculation (Fan et al. 1991). The structure and dimensions of $\boldsymbol{\Delta}$ and **M** in the RHS of (7) have been defined in Ricardez Sandoval et al. (2007). The outcome of (7) provides a bound (*k*) on the worst-case variability problem as well as the critical disturbance profile in each υ_q that generates this condition. However, these results are only valid around a nominal operating condition, specified by $\bar{\mathbf{u}}$, $\bar{\mathbf{y}}$, **d**, and $\boldsymbol{\lambda}$. Thus, the calculation has to be re-done around each set of nominal conditions arising during the optimization problem. Then, the process worst-case output variability is defined as follows:

$$\varphi^y = \bar{\mathbf{y}} + \max_{\mu_{\boldsymbol{\Delta}_y}(\mathbf{M}_y) \geq k^y} k^y \tag{8}$$

Where $\boldsymbol{\Delta}_y$, $\mathbf{M}_y$ and k^y represent the perturbation matrix, the interconnection matrix and a bound w.r.t. the output **y** given by (4), respectively. Based on the worst-case output variability, a cost can be assigned to estimate the process variability cost.

2.6 Process feasibility.

The approach taken to assess the worst-case output variability was also used to test that the process constraints are satisfied. This is referred to as process feasibility. To evaluate this condition, robust models like (2) and (4) have to be obtained from the disturbance ($\boldsymbol{\upsilon}$) to the process variable, e.g. **u**, which has to be kept within limits. Thus, (7) and (8) can be rewritten in terms of the process variables (**u**) as follows:

$$\bar{u} \pm \max_{\mu_{\boldsymbol{\Delta}_u}(\mathbf{M}_u) \geq k^u} k^u \leq 0 \tag{9}$$

Where $\boldsymbol{\Delta}_u$, $\mathbf{M}_u$ and k^u are the perturbation matrix, the interconnection matrix and a bound w.r.t. **u**. Inequality (9) is considered in the present analysis to guarantee feasibility during the process transient operation.

2.7 Optimization problem.

The mathematical expressions (1), (3), (8), and (9) can be combined into one optimization problem as follows:

$$\begin{aligned} &\min_{\boldsymbol{\eta}=[\mathbf{d},\bar{\mathbf{u}},\bar{\mathbf{y}},\boldsymbol{\lambda}]} \mathrm{CC}(\mathbf{d},\bar{\mathbf{u}}) + \mathrm{OP}(\mathbf{d},\bar{\mathbf{u}}) + \mathrm{VC}(\mathbf{d},\bar{\mathbf{u}},\boldsymbol{\lambda},\varphi^y) \\ &s.t. \quad \varphi^y = \bar{\mathbf{y}} + \max_{\mu_{\boldsymbol{\Delta}_y}(\mathbf{M}_y) \geq k^y} k^y \\ &\qquad \bar{\mathbf{u}} \pm \max_{\mu_{\boldsymbol{\Delta}_u}(\mathbf{M}_u) \geq k^u} k^u \leq 0 \\ &\qquad \mathbf{A}(w_k)^T \mathbf{Q} + \mathbf{Q}\mathbf{A}(w_k) < 0 \quad for \quad all\ w_k \in \mathbf{W} \\ &\qquad \boldsymbol{\eta}^l \leq \boldsymbol{\eta} \leq \boldsymbol{\eta}^u \end{aligned} \tag{10}$$

The above nonlinear constrained optimization problem constitutes the mathematical formulation proposed to simultaneously design and control chemical processes. Although the process model equations are not explicitly shown in (10), they are implicitly used to calculate the matrix **A** and **M**. The algorithm used to solve (10) has been given in Ricardez Sandoval et al. (2007). It should be noted that the present methodology assumes that the control structure and the process flow sheet are fixed a priori; that is, the control structure selection and the process synthesis problem are not considered in this study. These subjects may be included in (10) but is beyond the scope of this work.

3. TENNESSEE EASTMAN PROCESS

The methodology presented in the last section was applied to simultaneously design and control the Tennessee Eastman Process (Downs and Vogel, 1993). This process produces two liquid products (G and H) and one by-product (F) from four gaseous reactants (A, C, D and E) and one inert (B) using a two-phase exothermic reactor, a flash separator, a stripper, a centrifugal compressor, and a condenser. Based on the products' desired quality and production rate demands, this process has six modes of operations. The plant's open-loop transient behaviour can be simulated using a mechanistic model-based code provided by Downs and Vogel. The TEP was selected as a case study because is a challenging problem since it combines different units and it is open-loop unstable with rapid runaway behaviour. Thus, the process must be operated in closed loop. Due to the above, several stabilizing control strategies have been reported in the literature for this particular process. The present study used the decentralized control strategy proposed by Ricker (1996)

to assess the integration of design and control of the TEP. This control strategy was chosen because it can attenuate almost all the disturbances expected for the TEP. Also, a Simulink® code provided by Ricker (1996) is available to simulate the plant's closed-loop transient behaviour. Although Ricker's control strategy was developed for the plant's six modes of operation, only the base case operating mode was considered in the present analysis. The production targets specified for the base case are a product mass ratio of 50/50 (G/H) with a production rate of 7038 kg/hr for each product. Figure 1 shows the TEP flowsheet and the aforementioned control strategy which requires 17 PI controllers to stabilize the plant. The set point of the low level controllers, e.g. process input streams' flow controllers, are specified by the master level controllers' output, e.g. production rate controller, using ratio control. Details about this control structure have been given in Ricker (1996).

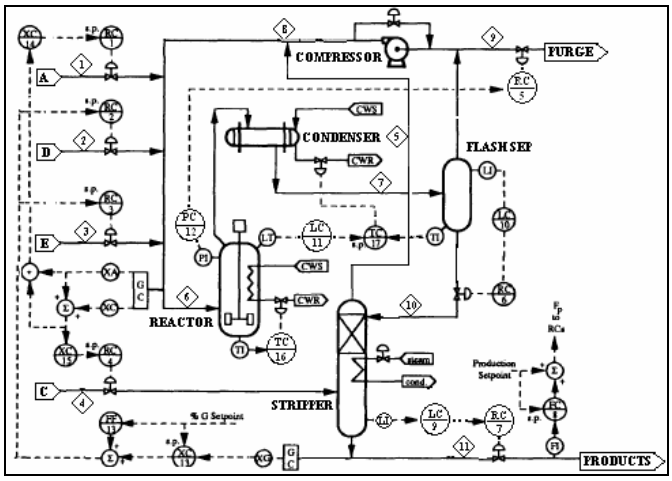

Fig. 1. Control strategy for the TEP (Ricker, 1996).

3.1 TEP cost function.

For the present study, the reactor, the flash separator, and the stripper were considered in the TEP cost function. Since the TEP code only provides the unit's capacities (ft^3), it was assumed that the units are vertical cylindrical vessels made of carbon steel with a length/diameter ratio of 4. Consequently, the bare-module cost, in 1982 USD, for each process unit can be expressed as follows (Seider et al., 1999):

$$C_{BM,unit} = 5946 D^{2.1}\left(19.82 - 12.55 \ln P + 2.36(\ln P)^2\right) \quad (11)$$

Where D is the vessel's diameter in meters and P is the pressure in bars. Assuming that the plant was built in 1992, the TEP annualized capital cost is defined as follows:

$$CC = r\left(C_{BM,reac} + C_{BM,sep} + C_{BM,strip}\right)(360/315) \quad (12)$$

Where r is the desired return on investment, assumed to be 20 %/yr. The TEP operating costs function for the base case is defined as follows (Downs and Vogel, 1993):

$$OP = PU*PUR + PS*PR + CO*CW + ST*STR \quad (13)$$

Where *PU*, *PS*, *CO*, and *ST* refer to the purge, the product stream, the compressor and the steam costs, and *PUR*, *PR*, *CW*, and *STR* refers to the purge rate, the product rate, the compressor work and the steam rate, respectively. The data used to estimate *OP* has been given in Downs and Vogel (1993). The TEP variability cost was defined as the difference between the cost of producing G and H under the effect of disturbances and transient conditions and the cost of producing both products at its target values and at steady state (ideal case). To ensure that the products meet the production mass flow rate demands (G* and H*), the products mass flow rate set point values ($\overline{G}$ and $\overline{H}$) have to be specified above its targets values. To estimate the products' mass flow rate worst-case variability w.r.t. $\overline{G}$ and $\overline{H}$, bounds on these two variables (k^G and k^H) are calculated by solving (8). Thus, the TEP variability cost function can be defined as follows:

$$\begin{aligned} VC &= cp_G \varphi^G + cp_H \varphi^H \\ \varphi^G &= \overline{G} + \max_{\mu_{\Delta_G}(\mathbf{M}_G) \geq k^G} k^G - G* \\ \varphi^H &= \overline{H} + \max_{\mu_{\Delta_H}(\mathbf{M}_H) \geq k^H} k^H - H* \end{aligned} \quad (14)$$

Where cp_G and cp_H denotes the costs for producing G and H and assumed to be both equal to 0.22 \$/kg. The functions φ^G and φ^H represent the worst-case variability in the products and reflect the additional amount of product (kg/hr) above the targets (G* and H*) that must be produced to satisfy the production demands in the presence of disturbances.

3.2 Disturbances.

The TEP code can be used to simulate the plant's behaviour under the effect of 20 different disturbances. For the present analysis, a bounded random variation in A, B, and C feed composition (stream 4 in Fig. 1) was chosen as the disturbance for which the TEP was designed. The bounds used for these disturbances were (mol %): ±0.01, ±0.003, and ±0.01 for components A, B, and C, respectively. This perturbation, named IDV-8, was chosen because it generates large variations in the flow rate of the products.

3.3 Robust closed-loop TEP model.

The present methodology is based on the accurate identification of a closed-loop linear state space model supplemented with model parameter uncertainty (2). For the TEP and the control strategy shown in Figure 1, robust models like (2) were obtained as follows: based on a Fast Fourier Transform (FFT) analysis of the original IDV-8, a PRBNS was designed for this disturbance and used to simulate the plant's closed-loop transient behaviour. The recorded input/output data is then used to obtain robust models like (2) applying the procedure explained in section 2.3. The closed-loop TEP has 41 available measurements, 9 set points, from which 5 are also process available measurements, and 12 manipulated variables, from which 3 were fixed to a constant value by Ricker's control strategy, i.e., agitator speed, recycle valve and steam valve. Thus, 54 robust models have to be identified for this process. For accurate systems identification, the predetermined plant's Gaussian noise was removed from the code and all the available process measurements were assumed to be continuous.

3.4 TEP stability, worst-case variability and feasibility.

The state space uncertain matrices $\mathbf{A}(\theta_A)$ in the identified state space models are used to evaluate the plant's stability using inequality (3). Thus, 54 inequalities like (3) have to be defined and evaluated to guarantee that the design is asymptotically stable. The TEP worst-case variability was defined in (14). To estimate k^G and k^H in (14), robust models like (2) and (4) have to be identified from the disturbance IDV-8 to the products production rate (stream 11 in Figure 1). The procedure to obtain (4) from (2) was given in section 2.5. The values of $\overline{G}$ and $\overline{H}$ in (14) are specified from optimization. Constraints on the products' quality and mass flow rate were considered to ensure products' specs. For example, product G's mass flow rate constraint was defined as follows:

$$\overline{G} - \max_{\mu_{\Delta_G}(\mathbf{M}_G)\geq k^G} k^G - G^* \geq 0 \qquad (15)$$

The quality constraint on G as well as the product H's constraints were defined as in (15). Also, six process operating constraints defined for the TEP were considered in the analysis. In addition, process measurements such as stream compositions and flow rates, and the process manipulated variables, have also to remain within bounds. These process constraints were defined as in (9); for example, the maximum reactor pressure constraint was defined as:

$$\overline{P} + \max_{\mu_{\Delta_P}(\mathbf{M}_P)\geq k^P} k^P - P_{\max} \leq 0 \qquad (16)$$

Where $\overline{P}$ denotes the reactor's nominal pressure, defined as a set point by the control strategy and whose value is specified from optimization; and P_{max} is the reactor's maximum allowed pressure. The rest of the constraints were defined in the same fashion and are not shown here for brevity.

3.5 Scenario-I: Reactor's design only.

In this scenario, only design changes for the TEP reactor were considered. The cost function was defined as sum of equations (12), (13), and (14) whereas the process worst-case variability was assessed from (14). To ensure process feasibility, constraints like (15) and (16) were defined for the process unit's operating constraints (pressure, temperature and level), the products flow rate (stream 11), the purge valve (stream 9) and the reactor cooling water flow rate valve. The decision variables for this problem were the reactor's capacity (ft^3), the tuning parameters (K_c and τ_I) of the reactor's pressure, level, and temperature controllers (PC-12, LC-11, and TC-16 in Fig. 1), the purge valve controller's tuning parameters (RC-5 in Fig. 1), the reactor's pressure, level and temperature set points, and the production rate set point. Problem (10) was rewritten in terms of the above specifications to obtain the reactor's optimal design. The resulting formulation was coded in MATLAB®. Table 1 shows the plant's current design and costs as well as those obtained for this scenario. As shown, the simultaneous design and control strategy found a design whose annual cost is approximately *11.6%* cheaper than the TEP current design. The strategy suggests an increment in the reactor's capacity that leads into significant savings in the plant's operating cost. The reduction in cost is mostly related to a reduction in a purge rate combined with a higher reactor's pressure set point made possible by the use of a larger reactor. To test the results, the closed-loop TEP model was simulated under the effect of the selected disturbance (IDV-8) using *Scenario-I*'s design parameters. As shown in Fig. 2A, product G's flow rate is always above the target specifications. It can also be shown that the rest of the constraints defined for this scenario remain feasible. Although *Scenario-I* produced an economically attractive design, the variability cost is slightly higher than the TEP current variability cost. This is because none of the controllers selected in *Scenario-I* are related to the products flow rate, specified as the production targets; in addition, the stripper is the last process unit before components G and H turn into products. Thus, consideration of the stripper in the design will have a significant effect on the product variability as shown in the next scenario.

3.6 Scenario-II. Reactor and Stripper's design.

Based on the above, *Scenario-I* was extended to include the stripper's design. The cost function, and the process variability function were the same as in *Scenario-I*. In addition to the process constraints defined for the previous scenario, a constraint on the stripper liquid product flow valve, (stream 11 in Fig. 1) was included. Besides *Scenario-I*'s decision variables, the stripper's capacity (ft^3), the stripper's level and liquid rate controller tuning parameters

(LC-9 and RC-7 in Fig. 1) and the stripper level set point were also considered as decision variables for this scenario. As in *Scenario-I*, the resulting formulation was rewritten in terms of these definitions and was coded in MATLAB®. As shown in Table 1, *Scenario-II*'s design is approximately *4.1%* more economical than *Scenario-I*'s design; this is mainly due to a reduction in *Scenario-II*'s variability cost, which comes from a tighter control on the products mass flow rates variability. Also, the results show that the stripper currently used might be overdesigned since a smaller stripper is calculated by *Scenario-II*'s design. Thus, the additions made to this scenario determined a more economical design with less production flow rates variability. *Scenario-II*'s design was simulated with the closed-loop TEP model and tested under the influence of IDV-8. As shown in Fig. 2B, product G's flow rate is above the target specifications with a narrower variability range if compared to Fig. 2A. The rest of the process constraints also remained within bounds.

Table 1. Comparison of TEP designs.

Variables	Current Design	*Scenario-I*	*Scenario-II*
Reactor (ft^3)	1300	1600	1600
Flash (ft^3)	3500	3500	3500
Stripper (ft^3)	156.5	156.5	120
CC ($/yr)	$8.69x10^4$	$9.06x10^4$	$9.02x10^4$
OP ($/yr)	$9.28x10^5$	$7.07x10^5$	$7.07x10^5$
VC ($/yr)	$3.71x10^5$*	$4.28x10^5$	$3.73x10^5$
Total Cost ($/yr)	$1.38x10^6$	$1.22x10^6$	$1.17x10^6$

*Obtained from 200 hrs. simulation.

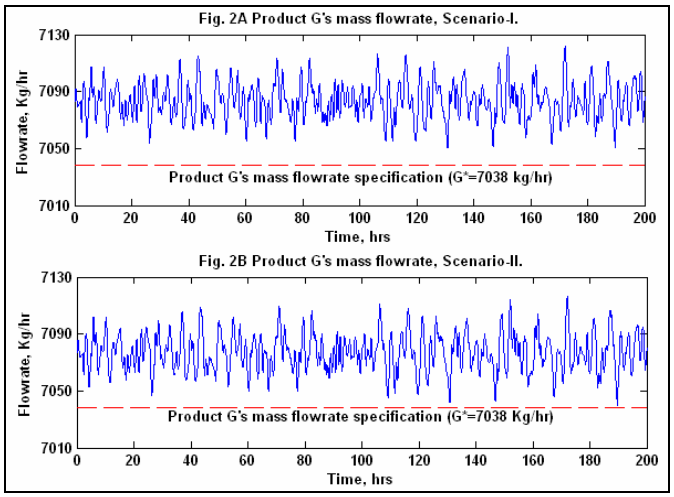

Fig. 2. Plant's simulation using the design parameters.

4. CONCLUSIONS

A methodology based on robust control tools has been used for the simultaneous design and control of the Tennessee Eastman Process. The results obtained by the proposed method show that the plant's actual design can be improved by resizing the process units. This redesign will lead to savings of at least *15.2%* in the plant's annual cost. The inclusion of additional perturbations as well as other process units within the TEP's design is under current analysis. The key advantage of the proposed approach is that it does not require dynamic programming which can be computationally expensive even for much simpler processes than the TEP process considered in this study.

ACKNOWLEDGEMENTS

The authors would like to acknowledge J.J. Downs from The Eastman Company, CONACYT from Mexico and NSERC.

REFERENCES

Boyd, S. and Q. Yang (1989). Structured and simultaneous Lyapunov functions for system stability problems. *Int. J. Contr.*, **49**, 2215-2240.

Chawankul, N., L.A. Ricardez Sandoval, H. M. Budman and P.L. Douglas (2007). Integration of design and control: A robust control approach using MPC. *Can. J. Chem. Eng.*, **85**, 433-446.

Downs, J.J. and E.F. Vogel (1993). A plant-wide industrial process control problem. *Comp. & Chem. Eng.*, **17**, 245-255.

Fan, M.K.H., A.L. Tits and J.C. Doyle. (1991). Robustness in the presence of mixed parametric uncertainty and unmodeled dynamics. *IEEE Trans. on Autom. Contr.*, **36**, 25-38.

Gerhard, J., W. Marquardt and M. Mönnigmann (2006). Towards robust design of closed-loop nonlinear systems with input state constraints. *IFAC proc. on ADCHEM*, 329-334. Gramado, Brazil.

Ljung, L. (1987). *System Identification, Theory for the User*. Prentice Hall, New Jersey.

Nagy, Z.K. and R.D. Braatz (2003). Worst-case and distributional robustness analysis of finite-time control trajectories for nonlinear distributed parameter systems. *IEEE Trans. on Contr. Syst. Tech.*, **11**, 694-704.

Ricardez Sandoval, L.A., H. M. Budman and P. L. Douglas (2007). Simultaneous process and control design of dynamic systems under uncertainty. *IFAC Proc. on DYCOPS*, **II**, 51-56. Cancun, Mexico.

Ricker, N.L. (1996). Decentralized control of the Tennessee Eastman challenge process. *J. Proc. Contr.*, **6**, 205-221.

Seider W.D., J.D. Seader and D.R. Lewin (1999). *Process Design Principles*. John Wiley & Sons, USA.

Sakizlis,V., J.D. Perkins and E.N. Pistikopoulos (2004). Recent advances in optimization-based simultaneous process and control design. *Comp. & Chem. Eng.*, **28**, 2069-2086.

Seferlis, P. and M.C. Georgiadis (2004). *The Integration of Process Design and Control.* Elsevier, Amsterdam.